

Appendix B—Nd:YAG Laser Stability Issues and Repairs

This appendix contains information regarding performance issues and repairs to the Quantel YG-661 Nd:YAG laser used in our laboratory from July 2004 until August 2009. The primary issues described here are incorrect installation of the laser, a damaged q-switch trigger circuit, a malfunctioning capacitor bank, and physical damage to the laser head. The first part of the appendix describes the symptoms exhibited by the laser that indicated malfunctioning equipment and improper setup. The second part describes the repairs made to the laser, and the improvement in laser performance. It is my hope that this information will be of value to future graduate students.

Introduction

Our interest in the energy and temporal stability of our laser light comes from the initial HO₂ + HCHO near-infrared (NIR) cavity ringdown spectrum (Figure B.1). The spectrum was much noisier than anticipated, making any spectroscopic or kinetics measurements impossible.

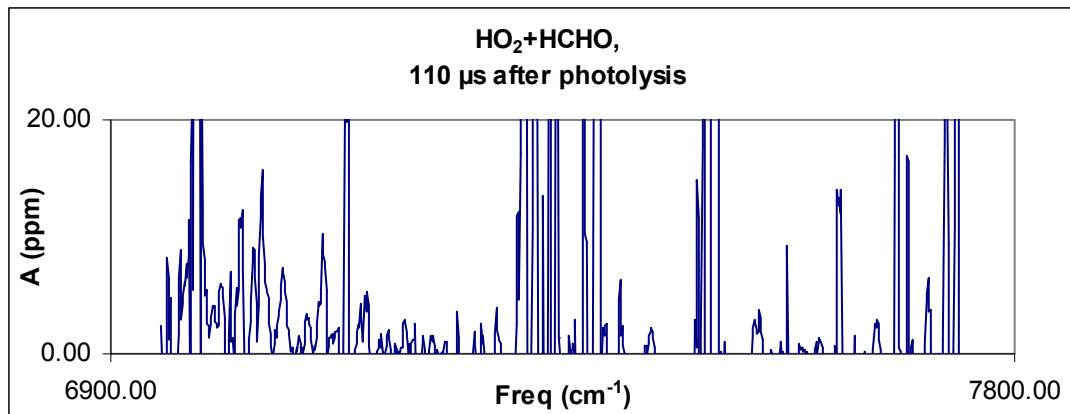


Figure B.1. NIR spectrum of HO₂ + HCHO products 110 μs after reaction. The considerable noise in the spectrum prevents accurate spectroscopy or kinetics measurements from being performed.

The apparent cause of this spectral noise was very large power fluctuations in the near infrared (NIR) light. Although cavity ringdown spectroscopy (CRDS) is theoretically independent of laser intensity (see Chapter 2), the data acquisition program will not operate properly if very large intensity fluctuations are present. The ringdown fitting program selects a voltage scale for the CompuScope board (CS1450) by measuring the peak voltage for one pulse, then recording 16 pulses on that voltage scale. Problems occur if the pulse that sets the scale is much lower in intensity than the other 16 pulses. If this problem occurs, the beginning of the averaged ringdown trace will be a saturated signal, and the expected exponential decay is only observed at the end of the signal.

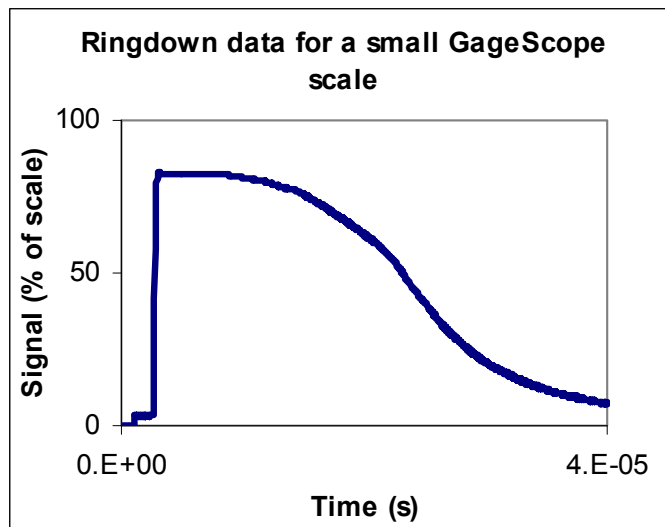


Figure B.2. Sample ringdown data acquired when the peak ringdown voltage exceeds the voltage scale of the CompuScope board. The first 25 μs has saturated signals averaged in. Exponential decay is only observed for the final 15 μs of the signal.

When we first observed this issue, it was unclear which optical component was causing the large intensity fluctuations. If any one piece of equipment (laser or optic) in the entire optical chain is malfunctioning, then the light reaching the detector will exhibit severe power fluctuations. Since the NIR light is generated through multiple nonlinear optical processes, we must check the power of light throughout the entire optical system (see Chapter 2 for a diagram of the entire system). The main places to check the light intensities are

- 1) The 1064 nm light emitted from the Nd:YAG oscillator and amplifier rods
- 2) The 532 nm light emitted from the second harmonic generator
- 3) The 640 nm light emitted from the dye laser (DCM dye)
- 4) The 1370 nm near IR light emitted from the H₂ Raman shifter

We used the methods described in Appendix A to collect 255 consecutive pulse energies at each point. We then analyze the energy distributions (and when possible, temporal distributions). These data tell us which part of the optical chain is causing the power fluctuations (YAG, dye laser, Raman shifter).

Initial Measurements and Classification of the Unrepaired Laser System

Energy Distribution Results and Analysis

The first data to examine are the distributions of pulse energies at two separate Nd:YAG flashlamp voltages. These data allow us to see how the distribution changes with average pulse energy, and allow us to correlate problems in one laser with problems in a previous laser. The energy distributions are illustrated in Figure B.3 for the YAG laser (a), dye laser (b), and NIR light (c). All data were taken at a flashlamp voltage of 1.28 kV. The measured photodiode or joulemeter voltage (x-axis) is directly correlated to the pulse energy, as described in Appendix A.

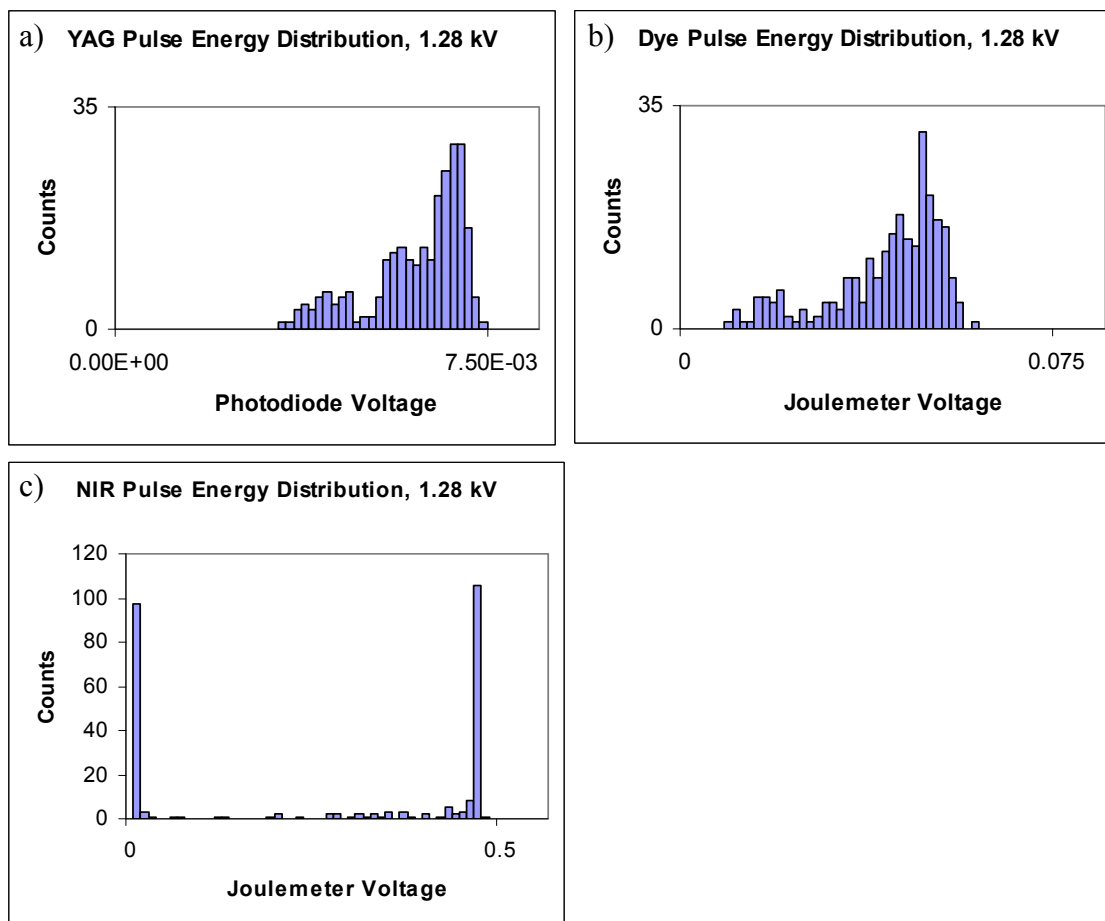


Figure B.3. Energy distributions for 255 consecutive pulses from the Nd:YAG laser (a), dye laser (b), and NIR light (c) at a flashlamp voltage of 1.28 kV. The YAG and dye distributions both have a main peak and a smaller peak at lower voltage. The NIR distribution shows a peak corresponding to saturation of the detector, and a large number of zero energy pulses. The number of “zero” counts in the NIR plot is approximately equal to the number of counts below the main peaks in the YAG and dye laser plots.

The YAG distribution contains 40 pulses (16%) in the low energy peak centered near 4 mV, 88 pulses (34%) in the midenergy peak centered near 5.6 mV, and 127 pulses (50%) in the high energy peak centered near 6.9 mV. Similar observations can be made for the dye laser pulses (50% of the pulses are in the high energy peak near 50 mV, while the other 50% are scattered below this peak). Finally, when we examine the NIR, we note

that roughly half of the pulses have near-zero intensity, while the other half saturate the detector.

Figure B.4 shows the energy distributions for the YAG, dye laser, and NIR light at 1.34 kV. At a higher flashlamp voltage, we expect the average pulse energy to increase, and the Nd:YAG laser to become more stable. We observed in Figure B.3 that the NIR light was saturating the detector. We therefore attenuated the light with a 99.98% reflective mirror to get a better idea of the actual energy distribution (Figure B.4d).

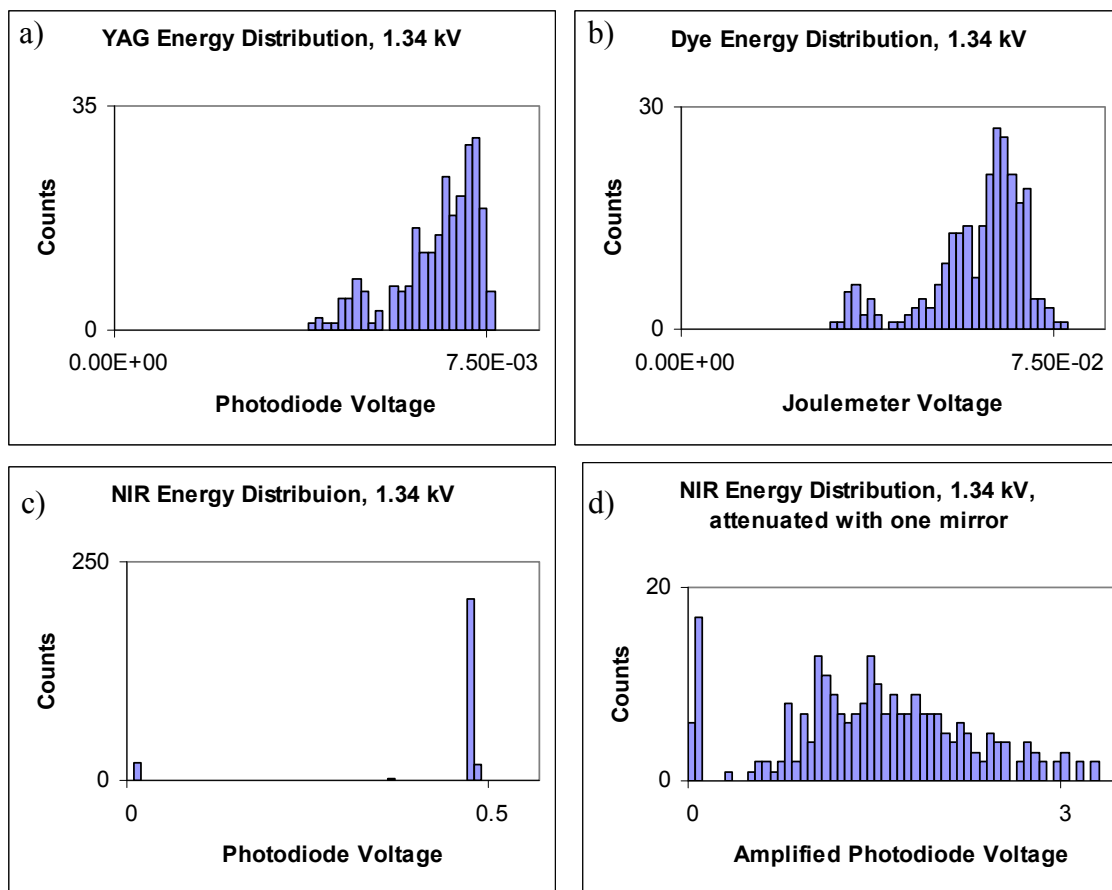


Figure B.4. Energy distributions for 255 consecutive pulses from the Nd:YAG laser (a), dye laser (b), and NIR light (c) at a flashlamp voltage of 1.34 kV. In order to get a better description of the NIR energy fluctuations, the NIR light was attenuated with one highly reflective mirror (d, $R = 99.98\%$), then amplified. The general shape of the YAG and dye distributions is the same as observed in Figure B.3. Although fewer zero energy pulses are observed in the NIR light, the energy distribution is very wide. The number of “zero” pulses in the NIR is nearly equal to the number of pulses in the smaller peaks of the YAG and dye distributions.

At the higher flashlamp voltage, we still observe the same two-peak features in the YAG and dye distributions. In the YAG distribution, there are 33 points (13%) in the small peak centered at 4.5 mV, while the rest of the pulses exceed 5.6 mV. Similar results are observed for the dye laser (21 pulses, or 8%, have a peak signal less than 40 mV). The NIR data show approximately 22 pulses (9%) with roughly zero intensity, and the

rest in a roughly Gaussian distribution. Figure B.4d shows that the NIR energy distribution is very wide, likely causing the GageScope scale problem described earlier.

Both the 1.28 and 1.34 kV distributions contain a cluster of low energy pulses in the YAG and dye laser, and roughly the same number of “zero intensity” pulses in the NIR distribution. **These data indicate that fluctuations in the YAG laser are causing the noise observed in the CRD spectrum.**

Temporal Distribution Results and Analysis

The conclusion from the energy distribution data was that fluctuations in the YAG are causing the energy drop-offs in the NIR. The question now becomes what is causing these energy drop-offs. One possibility is timing jitter between the firing of the flashlamps and opening of the Q-switch. Such timing jitter was observed on the GageScope while collecting energy data: the relative timing between the trigger and the pulse peak varied shot to shot. In theory, the laser should be controlled exclusively by two high precision digital delay generators (see Chapter 2). Since these delay generators were verified to be working properly, **the conclusion is that some part of the YAG is set up incorrectly.**

The first step to determining the cause of the laser pulse jitter is to characterize the time distribution of pulses. This can be done by reanalyzing the pulse distributions described above, but by picking out the timing of the peak rather than the peak voltage. It is possible to do this in Excel by judicious use of the `VLOOKUP` command. Note that the GageScope was triggered by the delay generators, so any measured distribution of times reflects a difference between flashlamp fire (controlled by the DDGs), and q-switch

opening (possibly controlled elsewhere). The timing analysis results are shown in Figure B.5 (flashlamp voltage of 1.28 kV) and Figure B.6 (flashlamp voltage of 1.34 kV)

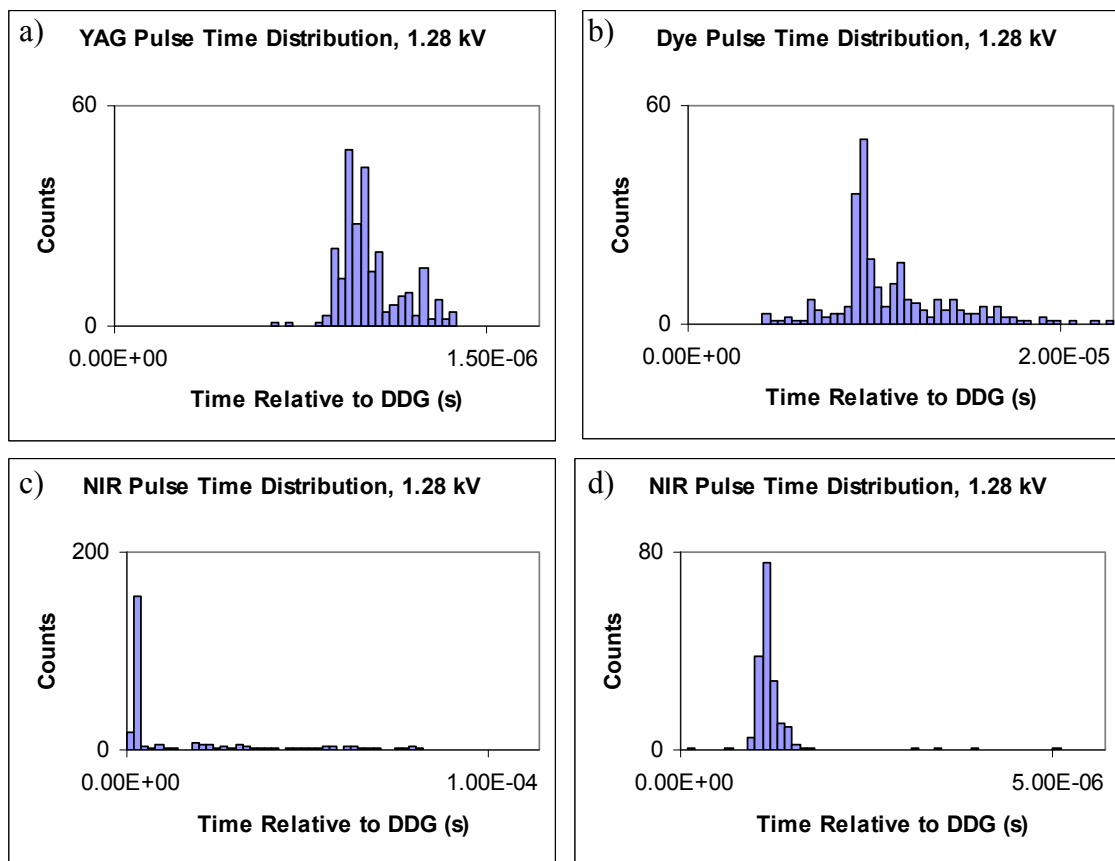


Figure B.5. Timing distributions for 255 consecutive pulses from the Nd:YAG laser (a), dye laser (b), and NIR light (c) at a flashlamp voltage of 1.28 kV. Pulse times are relative to the trigger signal from the DDG. In order to get a better description of the NIR timing fluctuations, we zoomed in on the first 50 μ s of the NIR distribution (d). The Nd:YAG distribution width is on the order of tens of nanoseconds, wider than expected.

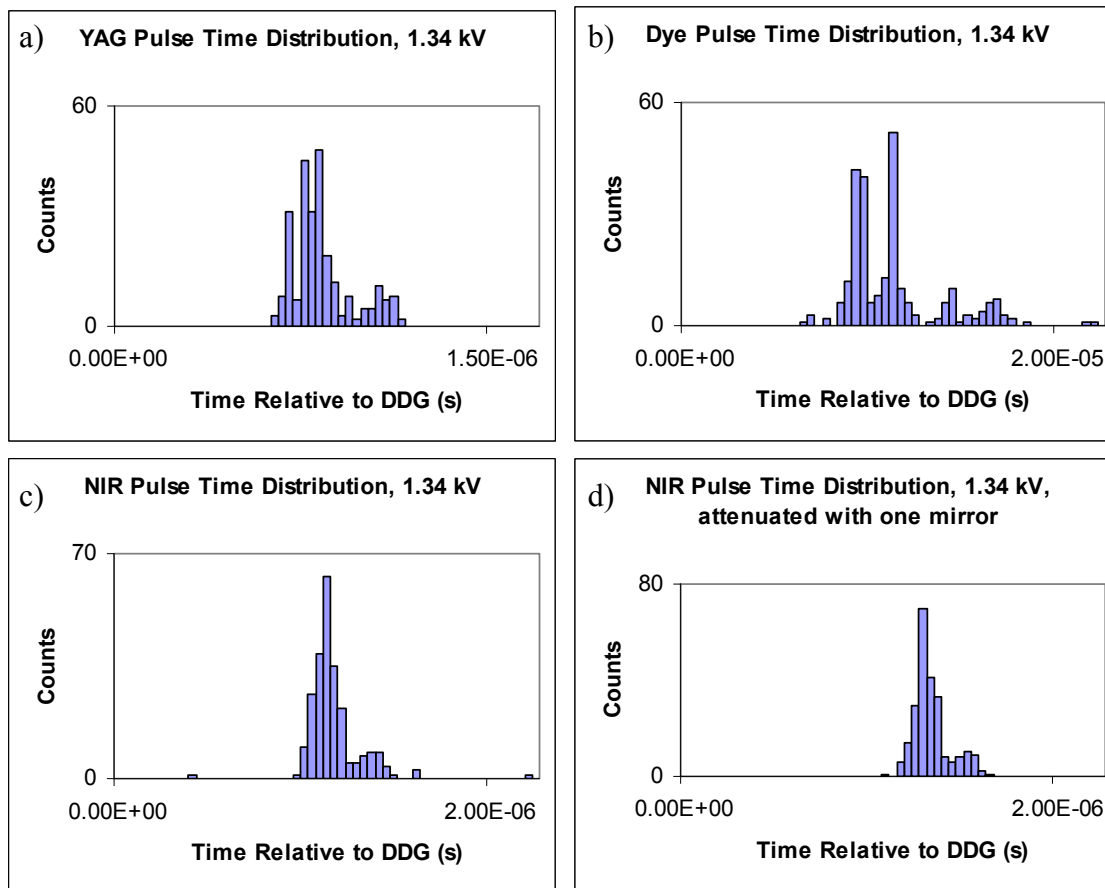


Figure B.6. Timing distributions for 255 consecutive pulses from the Nd:YAG laser (a), dye laser (b), and NIR light (c) at a flashlamp voltage of 1.34 kV. Pulse times are relative to the trigger signal from the DDG. The timing of the NIR pulses was not affected by the attenuation mirror (d). The Nd:YAG distribution width is on the order of tens of nanoseconds. Despite improvement compared to the 1.28 kV distributions in Figure B.5, this width is still larger than expected.

At 1.28 kV (Figure B.5), we notice that the YAG distribution contains a large main peak ($0.9 \mu\text{s}$), followed by a smaller peak out at later times ($1.2 \mu\text{s}$) containing 57 pulses (22%). The total width of the YAG distribution is on the order of $1 \mu\text{s}$. The dye distribution is much wider than the YAG distribution (on the order of $10 \mu\text{s}$), but the NIR distribution is similar in width to the YAG distribution. Similar results are observed at 1.34 kV (Figure B.6), though the YAG distribution appears to be somewhat narrower

than at 1.28 kV. At both voltages, the timing widths are much larger than the timing jitter in the laser specifications (7–9 ns).

We can also try to correlate when the laser pulse is emitted (from the timing distributions) with the energy of the pulse (from the energy distributions). Figure B.7 shows scatter plots of the pulse time vs pulse width for the Nd:YAG laser at 1.28 and 1.34 kV.

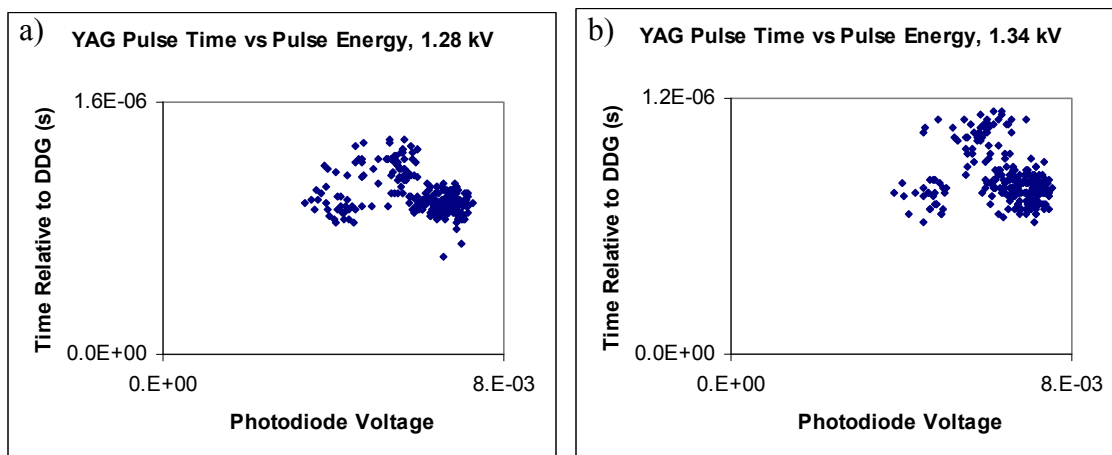


Figure B.7. Pulse timing vs pulse energy for the Nd:YAG laser at flashlamp voltages of 1.28 kV (a) and 1.34 kV (b). Three clusters of points are observed at both voltages, with the majority of points in the top cluster and lower right cluster. The clustering of points indicates a possible correlation between pulse time and pulse energy.

Both plots appear to contain three clusters of peaks. While it is hard to tell what the correlation is between pulse timing and pulse energy, the plots do indicate that the two concepts are somehow related based on the clustering. It appears that the majority of points lie in the top cluster and bottom right cluster, indicating a possible negative correlation. Regardless of the exact correlation, **the conclusion that we reach is that errors in when the q-switch opens is causing instability in pulse energy, and thus is the cause of the noise in the CRD spectrum.**

Laser Repair Information

Based on the pulse energy and timing analysis, we chose to re-examine how the q-switch was being triggered. We took the following six steps to improve the YAG timing and performance:

- First, the jitter between the Marx Bank signal and the DDG was measured, and was found to be unacceptably large. These measurements prompted us to trigger the Marx Bank directly from the DDG.
- The Marx Bank requires a 15 V trigger pulse, a larger voltage than our DDG can supply. Our second step was to build a pulse amplification circuit.
- Considerable ringing was observed on the charge and fire signal lines, so our third step was to repair and modify the optoisolator circuits for the charge and fire lines, as well as to add correct termination to the two lines.
- A 60 V spike was observed on all lines when the flashlamps fired. The cause of this spike was eventually identified as a problem with the YAG capacitor bank. Our fourth step was to swap the capacitor bank for a working spare bank.
- The cooling water running to the laser head during laser operation was observed to be warmer than 35 °C, the specified temperature. In order to correct this, our fifth step was to replace the “power pill” thermostat unit in the cooling unit.
- After making the first five changes, we still noticed that the energy out of the YAG laser would drop by 30% over the first two hours of operation, and continue to steadily drop afterwards. The cause of this is likely corroded o-rings and

buildup of minerals in the laser head. Our sixth step was to clean the laser head and replace all of the o-rings.

Jitter Between the Marx Bank Signal and the DDG

The original setup of our YG-661 had the Marx Bank being triggered by either the “Fixed Sync” or “Var Sync” outputs on the LU660 logic unit. However, this is not the correct way to trigger the Marx Bank. Normally, the Marx Bank is triggered by a different connection: the “J24” connector from the laser head cables. The normal setup allows for external triggering of the Q-switch (by passing an external signal directly through the laser), while the LU660 connection does not. The previous owners of the YG-661 set up the Marx Bank to be triggered by the LU660 because the signal out of J24 was being corrupted.

In “external mode,” the SB660 control box accepts a DDG trigger signal, and passes it directly through to the Marx Bank (as shown on the circuit diagram) via J24. We verified this by turning the laser off, and showing that the signal from the DDG is still passed through to J24. However, the laser would not fire when a 15 V signal was sent through J24, despite adjusting the timing of the Q-switch signal in relation to the flashlamp emission. Additionally, the laser would not fire when the Q-switch was controlled internally via J24, but *would* fire when controlled internally via the LU660. This led us to conclude that the signal out of J24 was being corrupted.

Finally, the Q-switch pulse out of the LU660 was compared to the DDG in order to determine the extent of jitter between the two. This jitter was on the order of microseconds, which is enough to explain the energy fluctuations previously observed.

We therefore conclude that the LU660 is an unacceptable Q-switch trigger. The Q-switch should be triggered directly by the DDG, ensuring a constant delay between flashlamp fire and opening of the Q-switch.

Amplification Circuit for the Marx Bank

Note: The Marx Bank used in our YG-661 is a Continuum Marx Bank, and DOES NOT MATCH the Marx Bank diagram in the YG-661 manual. These Marx Banks are a newer design, and information about them can be found in the NY-61 manual (YAG laser used in our other CRDS laboratory in Linde-Robinson).

The Marx Bank requires a 15 V positive edge trigger signal. The rise time of this signal must be fast (order of nanoseconds), and the signal shape must be stable from pulse to pulse in order to open the Q-switch at a constant time after the flashlamp emission. Unfortunately, none of the delay generators in the lab are able to provide a 15 V pulse. The Stanford DG535 delay generators in use can only provide a 4 V pulse. Likewise, the EG&G 9650 delay generators can only provide 10 V, and these generators do not work properly.

In order to obtain a 15 V pulse, we built an amplification circuit. The circuit takes a 4 V pulse from the DDG. This pulse is sent through a 6N137 high-speed optoisolator, and then series of two transistors in an emitter-follower configuration (VN10KLS first, then IRF510 second). In this circuit, the optoisolator will protect the DDGs from any energy spikes produced by the YAG. Additionally, the optoisolator will invert the DDG pulse. The two transistors will invert and amplify the pulse. The overall result of the circuit is that a 0–4 V square pulse is converted to a 0–15 V square pulse. We found that

using a slower optoisolator (such as a 6N135) or a slower first transistor would cause the rise time of the output pulse to be unacceptable. An 18 V power supply was connected to the drains of the two transistors, with a 515 Ω resistor between the 18 V line and the drain of the VN10KLS. A 5 V power supply was used to provide power to the 6N137.

Figure B.8 shows the full circuit diagram for the amplification circuit.

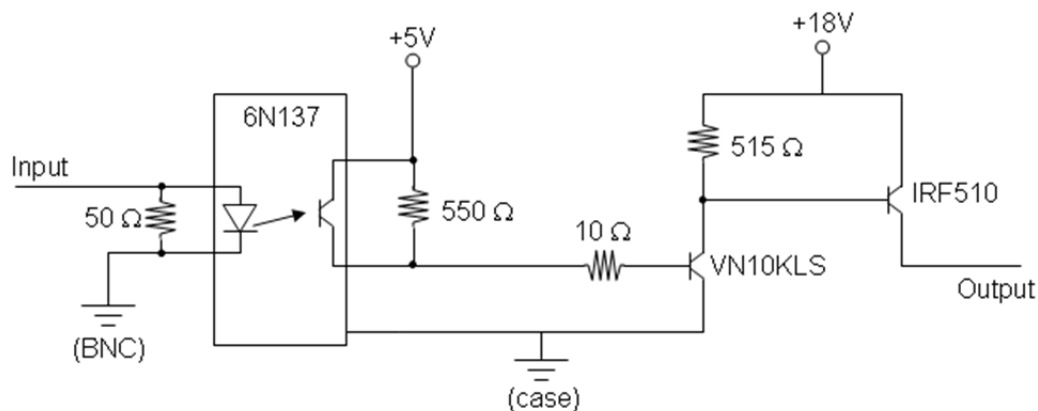


Figure B.8. Q-switch amplification circuit for the YG-661 laser. A 0–4 V square pulse is sent into a high speed optoisolator (6N137), then into two transistors in an emitter-follower combination (VN10KLS, IRF510). The output of the circuit is a 0–15 V square pulse.

The circuit performance was determined to be acceptable for use with our Marx Bank. The pulse rise time to 15 V was 400 ns (0–11 V in 100 ns). We also measured the firing of the Marx Bank inductively, by holding clip leads near the Marx Bank (flashlamps off), and observing the inducted pulse on an oscilloscope. The circuit was observed to trigger the Marx Bank properly.

Modifications to Charge and Fire Signal Lines

During the testing of the Marx Bank circuit, we also examined the flashlamp signals (charge and fire) being sent from the delay generator to the SB660 control unit via an optoisolator box. It is crucial that little or no noise is present on these lines, and that the signals being sent to the laser exhibit little to no timing jitter. Any corruption in these signals will lead to the flashlamps being fired at the incorrect time. Since the Marx Bank is being fired by the delay generator, the end result will be the Marx Bank being triggered at the “wrong” time relative to the flashlamps, resulting in a reduction in lasing power, or no lasing at all.

The charge and fire signals are first sent from the DDG to an optoisolator box. The outputs from the optoisolator box are then converted to a 9-pin D-sub connector, and fed into the SB660 supply box. Without the optoisolator box, DDG channels can be destroyed by electrical noise (this has happened in the past in 17 Noyes, when the laser was first installed in 2004).

After investigation of the optoisolator box, we observed two problems. First, the signals being sent out of the optoisolator box exhibited severe ringing. This was most likely due to the charge and fire lines not being terminated correctly. Second, the optoisolator circuit was wired up very poorly. Very thin wires were connected to balls of solder in midair to connect grounds to each other. Most of the components in the box were not mounted to a circuit board, making modification or repair to the circuit very difficult. Eventually, one of the two channels stopped working due to wires being disconnected and optoisolators burning out. Clearly a surface mounted circuit was needed, as well as correct termination for the optoisolator channels and output signals.

The new circuit for the optoisolator box is shown in Figure B.9. A positive DDG signal is sent into a 6N135 optoisolator. The output from this IC is sent into a 74128 NOR line driver to provide enough current to the Marx Bank. The output is terminated to 50 Ω at the D-sub converter box before being sent to the laser. All components are mounted to a circuit board. When this circuit is used for charge and fire signals, no ringing is observed.

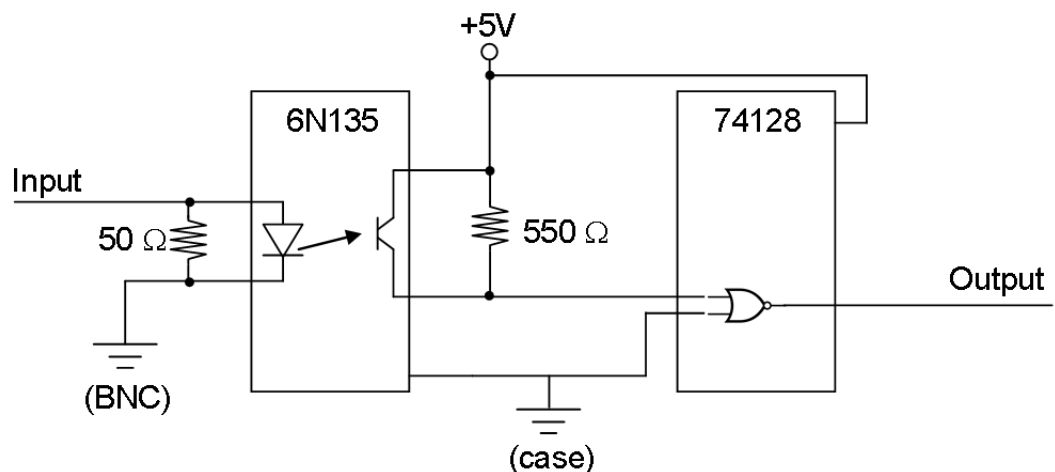


Figure B.9. Circuit diagram for the optoisolator box. The box contains two channels. Each channel has a copy of the above circuit. A 0–4 V square pulse is sent to a medium speed optoisolator (6N135). The pulse is then sent to a NOR line driver (74128). The output of the circuit is a 0–5 V square pulse.

The 60 V Spike and Replacement of the CB631 Capacitor Bank

Since installation of the YG-661 in 2004, a 15–60 V spike was observed on most of the laser lines (Charge, Fire, and “J24” Q-switch) at the time of flashlamp emission. This spike is not observed on the LU660 sync out. The amplitude of the spike is not affected by flashlamp voltage, varies shot to shot, and is always present at flashlamp emission. In the initial setup (Marx Bank triggered by LU660 sync out), this spike did not

affect lasing. However, the spike did cause a few DDG channels to be destroyed, prompting the creation of the initial optoisolator box.

The spike becomes a large problem when triggering the Q-switch via the DDG. When measuring the Marx Bank firing inductively using clip leads, we discovered that the Marx Bank was being triggered by the 60 V spike as well as our circuit. As a result, the Pockels cell was opening at the wrong time, and no lasing was observed. In order for the YG-661 to operate properly, the 60 V spike must be eliminated.

By swapping parts with another YG-661 (Jay Winkler's lab in the Beckman Institute), we determined that the original capacitor bank (CB631) was damaged. Changing capacitor banks for another CB631 results in the 60 V spike disappearing. We also showed that a third, smaller, capacitor bank (CB630) does not exhibit a 60 V spike at the time of flashlamp firing. It may be possible to repair the original CB631 by replacing the thyristor (C158PB). This part has been ordered and resides uninstalled in 17 Noyes; however, we will use the working CB631 in our laser for the time being. It is not possible to use the CB630 in the laser, because its capacitance (18 μF) is much lower than the CB631 (32 μF). The flashlamps would have to be turned up much higher when using the CB630, placing too much of a thermal strain on the Nd:YAG rods.

Replacing the Power Pill Thermostat

After the above repairs were performed, it was observed that the lasing power would decrease over time. Figure B.10 shows the energy per pulse of the 532 nm light from the YAG vs the amount of time that the flashlamps were firing. In the first three hours after the flashlamps were started, the energy out of the oscillator cavity would drop

by 30%. Even after the first three hours of flashing, the power would continue to steadily drop.

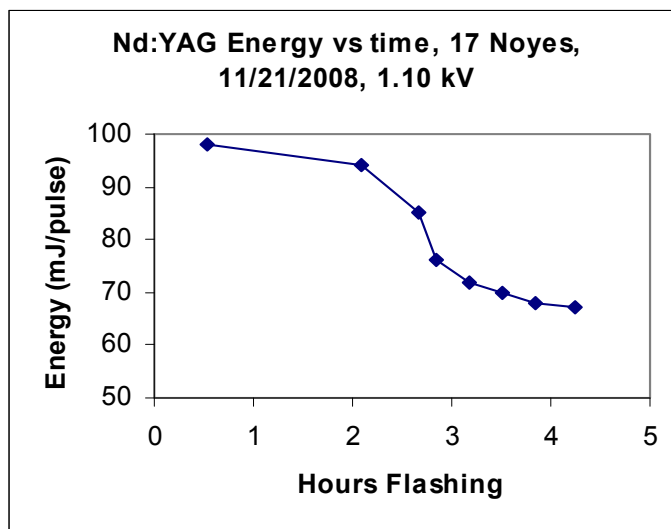


Figure B.10. Energy per pulse for the Nd:YAG vs flashlamp fire time. The plotted energies are for the 532 nm light; however, the same trend is observed for the 1064 nm oscillator light. Over the first three hours, the YAG energy drops by 30%. After three hours, the energy continues to slowly decrease.

Because the power out of the oscillator was behaving abnormally, we concluded that parts of the laser head needed to be repaired. Two ideas came to mind: incorrect cooling of the laser head (described in this section), and physical/chemical damage to the laser head (described in the next section).

The YG-661 manual specifies that for unseeded operation of the laser, the cooling water sent to the laser head should be no greater than 35 °C. If the water temperature exceeds this limit, then the YAG rods can overheat, changing the thermal lensing properties of the rods, leading to a reduction of lasing efficiency. We measured the cooling water temperature by placing a thermocouple into the DI reservoir. This reservoir

is located just prior to the laser head, so the reservoir temperature is a good measure of the water being sent to the YAG rods. Figure B.11 shows the temperature data.

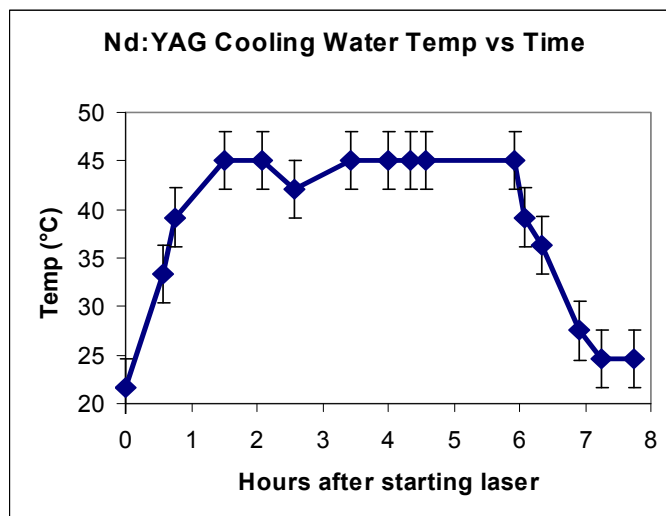


Figure B.11. Cooling water temperature in the Nd:YAG laser vs time since the laser flashlamps were started. The flashlamps were turned off 6 hours after starting the laser. During the time that the laser was flashing, the temperature rose to 45 °C and then stayed constant. Based on the voltage scale for the thermocouple, the uncertainty on each temperature measurement is ± 3 °C.

We notice that the water temperature increases to 45 °C over the first hour, then remains constant for the duration of laser operation. This temperature exceeds the manual’s specifications, so we must reduce the cooling water temperature in order to ensure proper operation of the laser. Note also that after 6 hours, the flashlamps were turned off, and the water temperature decreased back to room temperature.

The laser head is cooled by a reservoir of deionized water that exchanges heat with the building’s chilled water. The amount of heat transfer is controlled by changing the flow of the chilled water: if the deionized water becomes too warm, more chilled water is flowed to the heat exchanger. The flow of building water is controlled by a “power pill” thermostat: a ceramic thermostat with a wax reservoir and a small metal

extension separated by a flexible barrier. When the deionized water becomes too warm, the wax in the power pill melts. The expanding wax moves the barrier and forces the metal extension to press against a lever, increasing the flow of building chilled water to the heat exchanger. When the deionized water cools down, the wax resolidifies (and is compressed), the metal extension recedes, and the flow of building chilled water decreases. Each power pill has its own melting point, and therefore maintains one specific water temperature. The only way to change the cooling water temperature is to replace the power pill unit.

The power pill inside of our cooling unit was rated for 113 °F (45 °C) by the manufacturer. This power pill is appropriate for a seeded YAG, but not an unseeded one. By replacing the power pill with one rated for 95 °F (35 °C), we were able to reduce the laser head temperature back to 35 °C, the value specified in the manual.

Laser Head Cleaning and Replacement of O-rings

In addition to incorrect cooling, chemical deposits in the laser head or damage to the o-ring seals could also cause the 30% drop in energy over time observed in the previous section. If the head is coated with mineral deposits (formed from using impure deionized water), then the thermal properties of the head will change. The same principle holds for the o-ring seals: damaged or deformed o-rings will expand differently at elevated temperatures than undamaged o-rings. The end result for either problem is deviation from normal behavior in the physical and optical properties of the oscillator cavity at elevated temperatures. Therefore, it is critical to ensure that the laser head is clean, and that the o-rings are in good condition.

Upon opening the laser head, we noticed large calcium deposits on the ends of the head and inside the YAG rod reflector cavities. The o-rings were discolored and brittle, and likely had never been replaced since the laser was manufactured in 1989. We cleaned the laser head by disassembling as many parts as possible, then placing the laser head parts into household vinegar. The YAG rod reflector cavities were cleaned by dipping a cotton swab in vinegar, and lightly brushing the inside of the cavities. All of the o-rings inside of the laser head were replaced with new Viton o-rings (McMaster-Carr). After cleaning and replacing the o-rings, the laser head was reassembled and installed into the laser.

Result of Repairs

A full listing of the average energies and energy fluctuations as a function of flashlamp voltage for the repaired YG-661 laser can be found in Appendix A. In Table B.1, we present a comparison of the laser system performance before and after repairs (YAG, dye laser, Raman shifter). We immediately notice an improvement in both absolute energy and energy fluctuations. The pulse energy has increased by nearly a factor of three after repairs. The 1.2% fluctuation in 532 nm energy corresponds to a fluctuation of 0.5% at the oscillator rod, which matches the specs for the laser. We notice similar improvement in the dye laser output. The NIR light from the Raman shifter could not be measured at 1.24 kV prior to repair, but can be detected after repairs. The amount of NIR light produced (35 $\mu\text{J}/\text{pulse}$) is enough energy for use in cavity ringdown experiments.

Table B.1. Comparison of pulse energy and energy fluctuations at 1.24 kV for YG-661 (532 nm), dye laser (640 nm), and Raman shifter (1370 nm), before and after laser repairs

	E(YAG) (mJ/pulse)	σ_E/E_{avg} (YAG)	E(Dye) (mJ/pulse)	σ_E/E_{avg} (Dye)	E(Raman) (μ J/pulse)	σ_E/E_{avg} (Raman)
Before	78	41%	4.5	43%	— ^a	— ^a
After	225	1.2%	18	5%	35	29%

a) Energies too low to be measured

To get a better handle on the improvements in laser stability (both energy and timing), we can look at histograms of energy and pulse time with respect to the DDG, similar to those presented in Figures B.3–B.6. Shown below are histograms of energy (Figure B.12) and timing (Figure B.13) for the 1064 nm oscillator light, 532 nm light, dye laser light, and near-IR light. These plots were made at a flashlamp voltage of 1.25 kV.

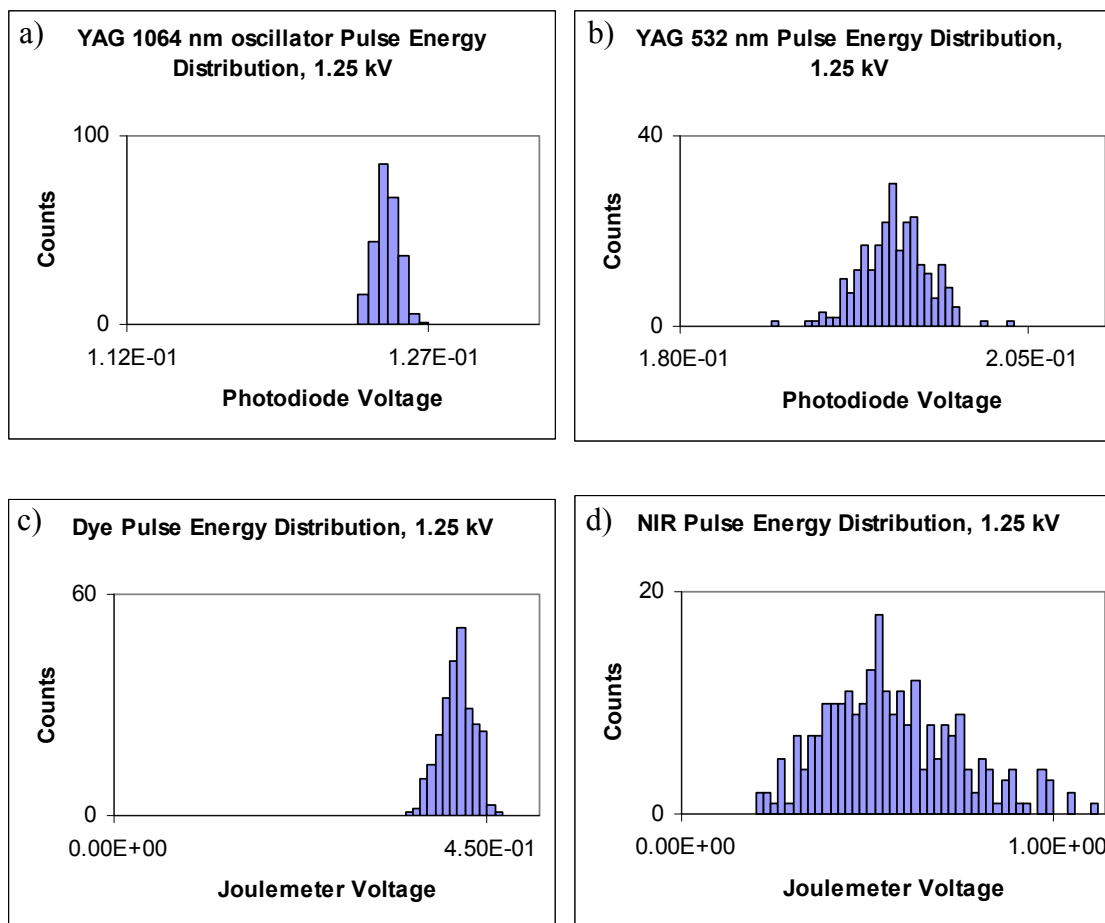


Figure B.12. Histograms of energy per shot for 255 pulses of 1064 nm oscillator light (a), 532 nm light (b), 640 nm dye laser light (c), and 7283 cm^{-1} near IR light (d). All light was collected at a flashlamp voltage of 1.25 kV. Plateau heights were analyzed for the 1064, 532, and 640 nm light, while peak height was analyzed for the 7283 cm^{-1} light. Note that the x-axis scales for the YAG light are much narrower than the axis scales in Figures B.3 and B.4. In comparison to Figures B.3 and B.4, no zero voltage pulses in NIR light are observed, nor is a bimodal distribution observed in YAG or dye laser light. Additionally, the width of the energy distributions appears to be narrower than in Figures B.3 and B.4.

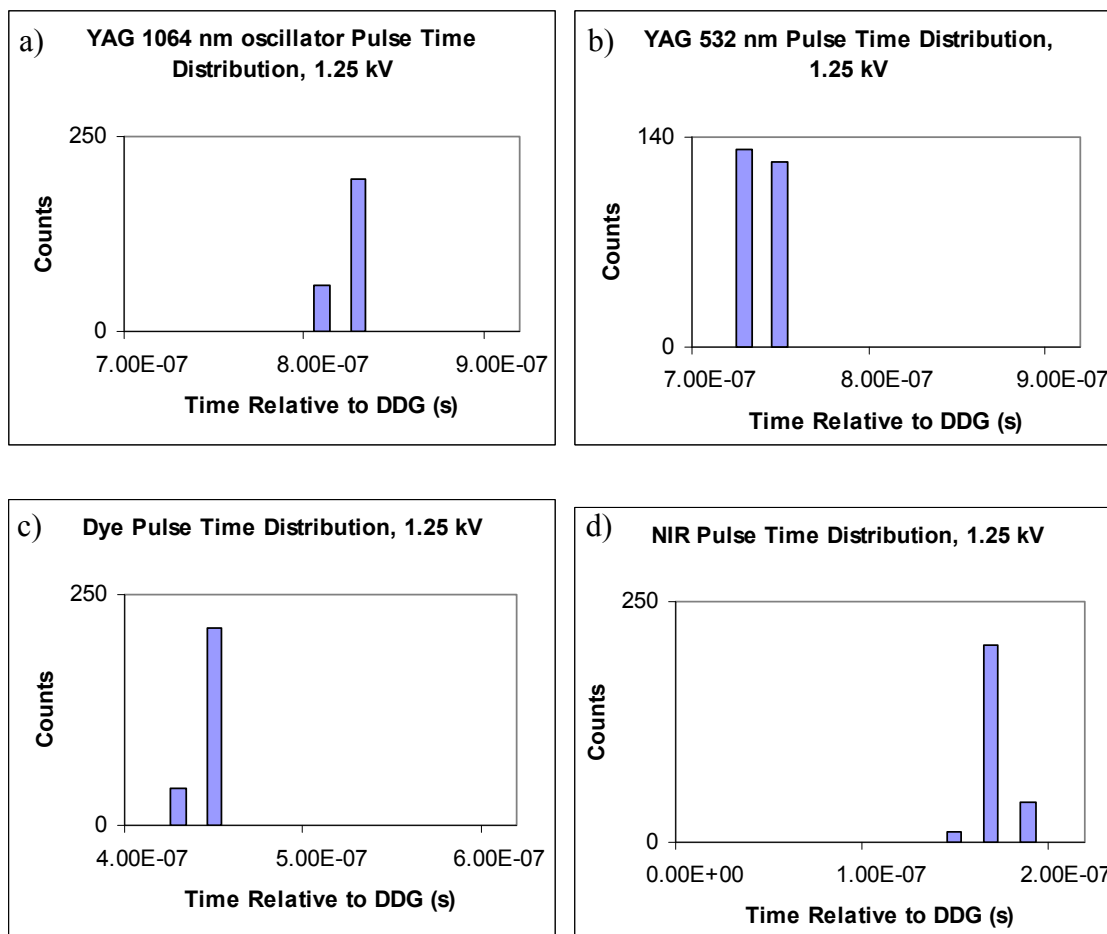


Figure B.13. Histograms of peak timing for 255 pulses of 1064 nm oscillator light (a), 532 nm light (b), 640 nm dye laser light (c), and 7283 cm^{-1} near IR light (d). All light was collected at a flashlamp voltage of 1.25 kV. In all plots, consecutive bars are 20 ns apart. This indicates that the jitter between pulses is shorter than the CompuScope sampling period of 20 ns. Further work with a higher sampling rate scope confirmed that timing jitter is less than 20 ns.

By comparing Figures B.12 and B.13 with Figures B.3–B.6, we notice two major improvements as a result of the laser repairs. First, the energy histograms reveal that the light at all stages (YAG, dye, NIR) has only one peak energy, as opposed to the original bimodal distributions. No zero energy pulses are observed in the NIR light, due to the reduced energy fluctuations in YAG and dye laser light. Second, the timing histograms show that the laser pulses have jitter of less than 20 ns at all stages (YAG, dye, NIR), a

vast improvement over the microsecond jitter in the unrepaired laser. Furthermore, our jitter now agrees with the YAG specification (8 ns). By using an oscilloscope with a higher sampling rate (2.5 GS/s, 0.4 ns between samples), we confirmed that the YAG jitter matched the 8 ns specification.

Conclusions

As stated repeatedly in this thesis, it is imperative that our cavity ringdown spectrometer's laser system is in proper working condition in order to obtain the best quality spectra possible. Incorrect installation of the Nd:YAG laser coupled with malfunctioning parts caused large power and timing fluctuations, leading to a reduction in the light pulse energy and unusable cavity ringdown spectra. By fixing the q-switch trigger circuits, capacitor bank, and laser head, we were able to repair the laser to a useful state. As a result, we observe increased absolute pulse energies out of the YAG, reduced pulse-to-pulse energy fluctuations, and a large reduction in timing jitter. The YAG laser now meets the manufacturer's specifications, an accomplishment given that the laser is 23 years old.

The take away lesson to future graduate students is to pay very close attention when installing new laboratory equipment, and to continually monitor the equipment's performance characteristics. Time should be taken to fix problems to the best of the student's ability, rather than performing quick workarounds that do not solve the problem, but merely ignore it. The YG-661 laser that was incorrectly set up was able to be used in a number of cavity ringdown spectroscopy projects including preliminary OH stretch spectra of the hydroxymethylperoxy radical discussed in Part 3 of this thesis. However,

the laser was performing far less than optimally, leading to ringdown spectra that were noisier than expected, and potentially rendering kinetics data useless. By spending the time determining the laser problems and fixing them, we were able to improve the quality of our data, and are now able to fully trust our kinetics measurements.